Available online at www.sciencedirect.com
ScienceDirect
Tetrahedron: Asymmetry
Tetrahedron: *Asymmetry* 18 (2007) 750–758

Dimer formation of cinchonidine in liquid phase: relevance to the heterogeneous catalytic enantioselective hydrogenation of ethyl pyruvate

József L. Margitfalvi,[a,*] Emilia Tálas,[a] Ferenc Zsila[b] and Sándor Kristyán[a]

[a]*Department of Organic Catalysis, Institute of Surface Chemistry and Catalysis, Chemical Research Center, Hungarian Academy of Sciences, 1025 Budapest, Pusztaszeri út 59-67, Hungary*
[b]*Department of Molecular Pharmacology, Institute of Biomolecular Chemistry, Chemical Research Center, Hungarian Academy of Sciences, 1025 Budapest, Pusztaszeri út 59-67, Hungary*

Received 6 February 2007; accepted 13 March 2007

Abstract—Literature data related to the possible dimer formation of cinchona alkaloids in the liquid phase are collected and analyzed. These data are correlated with experimental results obtained in the heterogeneous catalytic enantioselective hydrogenation of ethyl pyruvate. In this reaction, the addition of achiral tertiary amines (ATAs) resulted in an increase in both the reaction rates and enantioselectivity. The positive influence of ATAs was attributed to the suppression of dimer formation in aprotic solvents. The results of circular dichroism spectroscopy and ab initio calculations provided further proof for dimer formation. Four possible cinchonidine dimer configurations were found with approximate 11–13 kcal/mol stabilization energies.

1. Introduction

Cinchona alkaloids are widely used in various organic reactions to induce enantio-differentiation.[1,2] The crystallographic structure of cinchonidine has shown that intermolecular H bonds exist between the tertiary nitrogen atom of the quinuclidine moiety of the molecule and the OH group at C9 carbon.[3] There are additional literature data with respect to the intermolecular interactions between cinchona alkaloid molecules in solution.[4–10]

In non-polar solvents, the N···HO bonds lead to the weak association of alkaloid molecules forming dimers. Direct evidence of dimer formation have been obtained by circular dichroism spectroscopy. Circular dichroism spectra of cinchona alkaloids shows an exciton type Cotton effect at 230 nm band of free bases (0.4 mM) in CH_2Cl_2 or dioxane, but not in MeOH. Cupreines with two OH groups show a stronger effect.[4]

Upon using osmometry to determine the average molecular weight of quinine in toluene solution (0.016 M, 37 °C), the presence of moieties larger than monomeric quinine has been detected. However, at lower concentrations than 0.004 M, the quinine was almost completely monomeric.[5]

The appearance of a cinchona solute–solute interaction has also been suggested based upon NMR investigations of racemic and enantiomerically pure dihydroquinine.[6] The NMR spectra of optically active dihydroquinine and of racemic dihydroquinine are significantly different when taken at 0.35 M in deuterochloroform. By using CD_3OD solvent, the difference in spectra was strongly reduced. The acetates of optically active and racemic dihydroquinine have also shown much smaller differences than dihydroquinine itself.[6] The auto-association product of quinine in chloroform solution has been established by investigating the temperature and concentration dependence of the NMR spectral parameters by combination of 2D NOESY and proton-selective relaxation rate measurement.[7] According to the latter results, quinine mainly exists as a dimer and the mole fraction of dimer is about 40% at a higher concentration (0.6 M). The conformation of the alkaloid is similar in the dimer and monomer. It

* Corresponding author. Tel.: +36 1 438 1163; fax: +36 1 325 7750; e-mail: joemarg@chemres.hu

0957-4166/$ - see front matter © 2007 Elsevier Ltd. All rights reserved.
doi:10.1016/j.tetasy.2007.03.012

has been proven that the quinuclidine ring is located on the quinoline ringside and the >CHOH moiety is on the other one. Moreover, the quinoline plane almost bisects the angle H–C9–OH. It is interesting to note that in these dimers, the quinoline parts of the two molecules exhibit almost parallel positions and no intermolecular N···HO interaction has been described. In toluene solution, species with a multiple weight of cinchonidine monomer have also been detected by mass spectrometry.[8]

The association of cinchona alkaloids has also been investigated by Fourier transform infrared (FTIR) spectroscopy.[9] In a solution of 0.01 M acetic acid in dichloromethane, a weak broad band above 3150 cm^{-1} was detected, which can be attributed to the formation of N···HO hydrogen bonds between two cinchonidine molecules (self association). The aggregation phenomenon of cinchonine in aqueous solutions was observed and analyzed via 2D FT-Raman spectroscopy. The aggregation is effective in the range where cinchonine is singly protonated at the quinuclidine nitrogen.[10]

Cinchonidine is one of the most active chiral modifiers in the asymmetric hydrogenation of α-ketoesters.[11,12] Even at very low alkaloid concentration (1.2×10^{-5} M), high enantiomeric excesses (80–85%) can be achieved.[13] However, the effective amount of cinchonidine in enantioselective hydrogenation is only a small portion of the total amount introduced into the system. The cinchonidine itself undergoes hydrogenation forming dihydro-, tetrahydro-, hexahydro-, and further hydrogenated derivatives.[14–16] It should be noted that 10,11-dihydro-cinchonidine is the most active chiral modifier among the hydrogenation products, hexahydro and dodecahydro derivatives show much less activity or they are practically inactive in asymmetric induction[17,18] carried out in toluene. The dependence of the reaction rate and enantiomeric excess on the modifier concentration has been investigated in great detail.[13,19] In this enantioselective hydrogenation reaction, the modifier–modifier interaction has also been considered to interpret the non-linear phenomenon observed under hydrogenation of ethyl pyruvate (EtPy) in the presence of equimolar amounts of cinchonidine and quinidine.[20]

Upon using cinchonidine as a chiral modifier in the hydrogenation of (*E*)-α-phenylcinnamic acids over Pd/TiO_2 Nitta has reported that achiral amine additives improve the enantiomeric excess. The presence of the amine was supposed to promote desorption of the product from the modified sites of the catalyst.[21,22] We have seen that in the enantioselective hydrogenation of EtPy over cinchonidine–Pt/Al_2O_3 catalyst system, achiral tertiary amines (ATAs), such as Dabco (1,4-diazabicyclo-[2.2.2]octane), triethylamine (TEA), and quinuclidine, increase both the reaction rate and the enantiomeric excess.[13,23] However, this phenomenon, called as 'ATA effect', appears only at low cinchonidine concentration and in non-polar solvents. The 'ATA effect' observed in toluene was attributed to the virtual concentration increase of the chiral modifier.[23] In the presence of ATAs, the equilibrium between the dimer and monomer forms of cinchonidine is shifted toward formation of the monomer. The 'ATA effect' was also observed in the enantioselective hydrogenation of α,β-diketones.[24]

Results described above provide a strong indication that cinchona dimers probably may exist in solution. However, to our knowledge there is no combined study related to the formation and characterization of cinchonidine dimer and its possible role in a catalytic reaction.

Herein, we report our attempts to obtain further information on the 'ATA effect' in the heterogeneous catalytic asymmetric hydrogenation of EtPy and to find a correlation between the presence of cinchonidine dimers and the increased enantioselectivity. For the accomplishment of the above goal, catalytic measurements have been performed and circular dichroism spectroscopy has been applied. Furthermore, molecular mechanics and ab initio calculations have also been used for the calculation and modeling the possible conformations of cinchonidine dimers.

2. Results and discussion

Kinetic data of the hydrogenation of EtPy over the cinchonidine–Pt/Al_2O_3 catalyst system in the absence and in the presence of different ATAs are summarized in Table 1 and Figure 1. As can be seen form these results (see runs 1 and 3 in Table 1), the addition of quinuclidine to the reaction mixture slightly increases the rate of racemic reaction. Based on the literature data, a nucleophile catalytic effect of tertiary amines can be suggested,[25] however, partial removal of poisoning oligomers from the platinum surface[26] could also be an alternative explanation, as it is known that pyruvate esters can form various oligomers and polymers on the Pt surface.[27]

Table 1. Influence of different tertiary amines on the reaction rate and enantiomeric excess in the enantioselective hydrogenation of EtPy

No.	ATAs	k_1 (min^{-1})	k_2 (min^{-1})	ee_{max}	ee_{end}
1	None[a]	0.0045	0.0068	—	—
2	None	0.0236	0.0747	0.838	0.819
3	Quinuclidine[a]	0.0077	0.0109	—	—
4	Quinuclidine	0.0482	0.0997	0.901	0.882
5	Dabco	0.0486	0.1267	0.909	0.905
6	MPD	0.0322	0.0989	0.895	0.872
7	TEA	0.0300	0.0905	0.849	0.843
8	Edcha	0.0220	0.0735	0.850	0.785
9	Edipa	0.0243	0.1280	0.824	0.796
10	3-Quinuclidinol	0.0468	0.0867	0.888	0.870
11	No[b]	0.0409	0.1268	0.945	0.945
12	Quinuclidine[b]	0.0699	0.1518	0.946	0.946

$[EtPy]_0 = 1.0$ M, [cinchonidine] $= 1.2 \times 10^{-5}$ M, ATA $= 6 \times 10^{-5}$ M, $T = 20$ °C, $p_{H_2} = 50$ bar, reaction time = 90 min, solvent = toluene, catalyst: 0.125 g 5 wt % Pt on Al_2O_3 (Engelhard 4759), 500 rpm, coinjection of ATA, EtPy: ethyl pyruvate, Dabco: 1,4-diazabicyclo-[2.2.2]octane, MPD: 1-methylpiperidine, TEA: triethylamine, Edcha: *N*-ethyldicyclohexylamine, Edipa: *N*-ethyldiisopropylamine. k_1, k_2: first order rate constants calculated from experimental points measured in the first 10 min and between 25 and 60 min, respectively.

[a] In the absence of cinchonidine.

[b] Solvent = 1 M acetic acid in toluene.

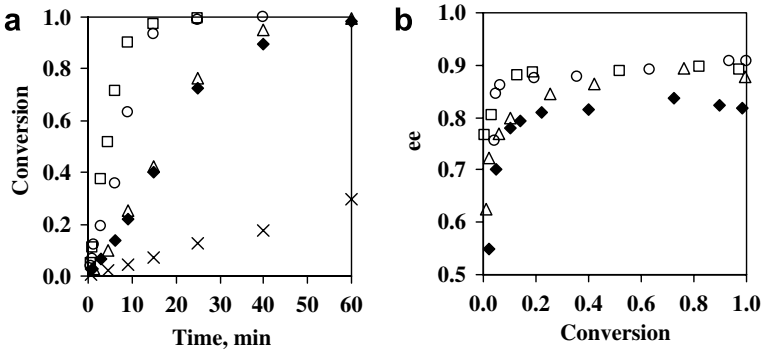

Figure 1. Hydrogenation of ethyl pyruvate (EtPy) in the presence of active ATAs. $[EtPy]_0 = 1.0$ M, $T = 20$ °C, $p_{H_2} = 50$ bar, solvent = toluene, catalyst = 0.125 g 5 wt % Pt on Al_2O_3 (Engelhard 4759), 500 rpm, coinjection technique. $[cinchonidine] = 1.2 \times 10^{-5}$ M, $[ATA] = 6 \times 10^{-5}$ M. ×—no cinchonidine, no ATA; ◆—no ATA; △—1-methylpiperidine (MPD); ○—quinuclidine; □—Dabco.

Data in Table 1 show that ATAs can be divided into two groups: effective and non-effective achiral tertiary amines. In the experiments carried out in toluene as a solvent with 1.2×10^{-5} M cinchonidine as a chiral modifier a five-fold amount of quinuclidine, Dabco or 1-methylpiperidine (MPD), increased the enantioselectivity by 5–10%. In this range of enantioselectivity, this increase is considered to be a substantial one. It is interesting to note that the addition of these ATAs resulted in a significant increase in the reaction rates (see Table 1 and Fig. 1a). 3-Quinuclidinol behaved similarly to other ATAs, while TEA resulted in lower activity and ee values. However, the addition of *N*-ethyldicyclohexylamine (Edcha) and *N*-ethyldiisopropylamine (Edipa) caused a slight decrease in the ee values. The results unambiguously indicate that effective ATAs have a more or less rigid structure, while non-effective ATAs have large alkyl substituents rotating freely and bonded to the tertiary nitrogen. These facts suggest the importance of steric factors in the 'ATA effect'.

It should be mentioned that the ATA effect appears also in methylcyclohexane solvents (results are not shown). Five-fold amounts of quinuclidine resulted in a 16% increase of ee and the k_1 and k_2 rate constants were increased 3.5 and 1.7 times, respectively.

In acetic media, quinuclidine has resulted in an increase in reaction rate but has no influence on the ee value. The reason for this observation is the high ee value (ee = 95%) in both experiments (see runs 11 and 12 in Table 1). These observations show again that the ATA effect is strongly solvent dependent, but nucleophile catalysis can be responsible for the observed rate increase. Figure 2 indicates that no noticeable rate and enantiomeric excess increase can be observed upon using ethanol as a solvent. It is in good correlation with the fact that the formation of cinchonidine dimers in ethanol has never been evidenced.

In the following series of experiments the behavior of two chiral modifiers, cinchonidine and 9-methoxy-cinchonidine (MeO-cinchonidine) (see Scheme 1) was compared. In the absence of ATA, MeO-cinchonidine resulted in a higher enantiomeric excess than cinchonidine (see Fig. 3a). Upon

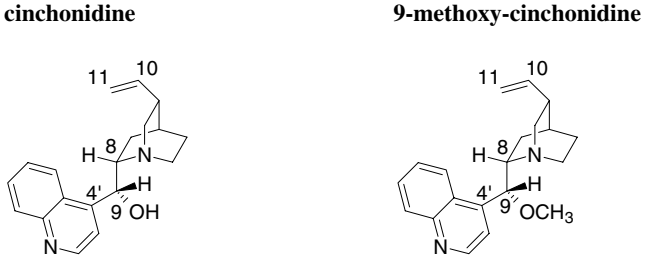

Scheme 1.

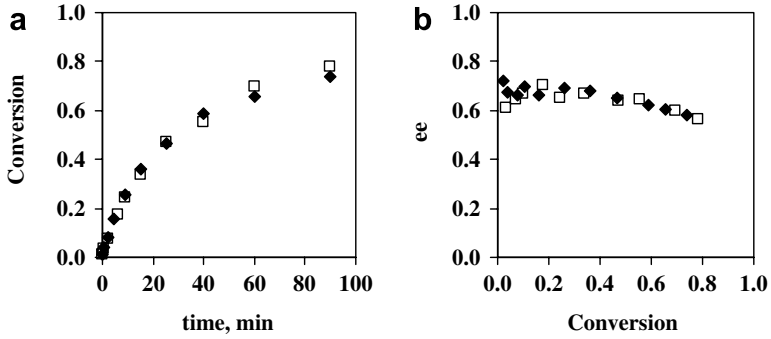

Figure 2. Effect of quinuclidine on the hydrogenation of ethyl pyruvate (EtPy) in ethanol solvent. $[EtPy]_0 = 1.0$ M, $[cinchonidine] = 1.2 \times 10^{-5}$ M, $T = 20$ °C, $p_{H_2} = 50$ bar, catalyst = 0.125 g 5 wt % Pt on Al_2O_3 (Engelhard 4759), 500 rpm, copremixing technique. ◆—no quinuclidine; □—6×10^{-5} M quinuclidine.

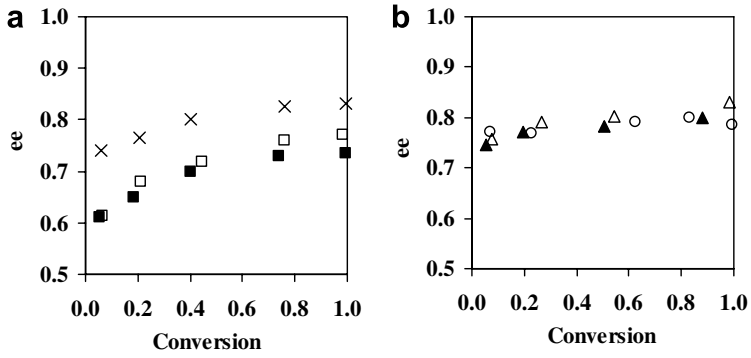

Figure 3. Effect of Dabco in the presence of different chiral modifiers. $[Etpy]_0 = 1.0$ M, $T = 20$ °C, $p_{H_2} = 10$ bar, solvent = toluene, catalyst: 0.02 g 5 wt % Pt on Al_2O_3 (Engelhard 4759), $V_{reaction} = 10\ cm^3$, copremixing technique. (a) 1.2×10^{-5} M cinchonidine; (b) 1.2×10^{-5} M 9-methoxy-cinchonidine. □, ■—no Dabco, two parallel experiments; ×—6×10^{-5} M Dabco; △, ▲—no Dabco, two parallel experiments; ○—6×10^{-5} M Dabco.

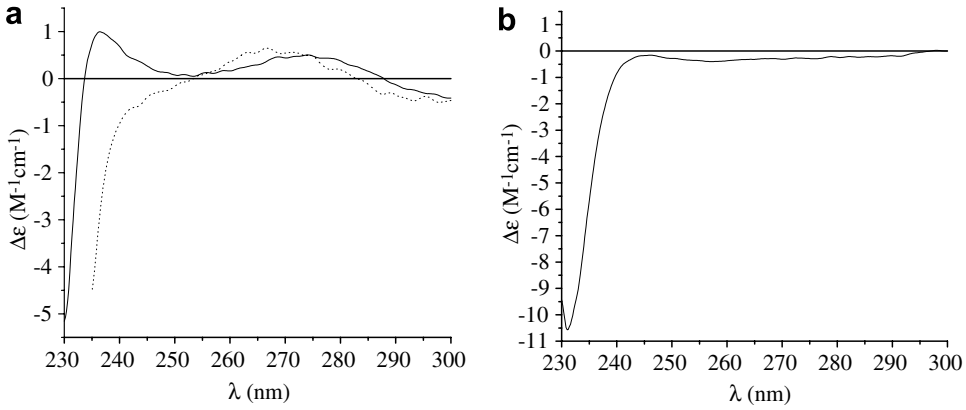

Figure 4. Circular dichroism spectra of chiral modifiers: (a) cinchonidine; (b) 9-methoxy-cinchonidine. Solid line—in dichloromethane; dashed line—in ethanol.

using cinchonidine, a significant increase in ee values was observed in the presence of Dabco (see Fig. 3a). However, upon using MeO-cinchonidine, no changes in ee values were observed in the presence of Dabco (see Fig. 3b). This is in good agreement again, with the fact that MeO-cinchonidine is not able to form a cinchonidine dimer via H bond formation. All these results strongly indicate that upon the addition of effective ATAs to cinchonidine, the increase in both the reaction rates and the enantioselectivity can be related to the virtual concentration increase of the monomeric form of cinchonidine. This form is considered as the active form of the modifier in this enantioselective hydrogenation reaction. This interpretation fairly explains the excellent performance of MeO-cinchonidine as observed by different authors.[18,28] However, no reasonable explanation has been given so far for the observed outstanding performance of MeO-cinchonidine.

To confirm the above explanation, circular dichroism measurements were carried out. Upon using time mode detection at 237.6 nm, the influence of achiral amines such as quinuclidine, Dabco, and TEA, on the supposed dimer sign were studied. From the oppositely signed exciton Cotton effects originating from the cinchonidine dimers the positive one is centered at 236.4 nm, while the negative wing is masked by another non-excitonic intense negative signal extending below 230 nm (Fig. 4a).[4] It should be noted that toluene cannot be used as a solvent because of its high absorbance values in that region. As can be seen from the data given in Table 2, in the case of aprotic solvent (CH_2Cl_2) the higher the concentration of ATA, the lower the indication of the dimer. However, as shown in Figure 4a, no exciton circular dichroism sign of cinchonidine dimers appeared in the ethanol. Upon using MeO-cinchonidine, the positive exciton sign did not appear either in the dichloromethane (Fig. 4b) or in the methylcyclohexane solutions. These observations have allowed us to conclude that the dimer forms of cinchonidine containing an N···HO interaction should exist under the conditions of asymmetric hydrogenation of EtPy. The shift of the equilibrium of the dimer from to the monomer one plays an important role in both the rate increase and the improved enantioselectivity. Consequently, the ATA effect can be related to the suppression of the dimer formation in aprotic solvents.

3. Computation modeling of the cinchonidine dimers

To computationally study the structure of dimers, we considered the *open* form of cinchonidine, for the reason that this form is the most stable in the liquid phase.[29] However,

Table 2. Effect of ATA on the circular dichroism data of cinchonidine

No.	ATA added	Concentration of ATA ($\times 10^{-3}$ M)	ATA–cinchonidine molar ratio	Solvent	$\Delta\varepsilon$ (M^{-1} cm^{-1})
1	None	—	—	Ethanol	—
2	None	—	—	CH_2Cl_2	0.94
3	Quinuclidine	0.4	1	CH_2Cl_2	0.91
4	Quinuclidine	0.8	2	CH_2Cl_2	0.74
5	Quinuclidine	2.0	5	CH_2Cl_2	0.70
6	Quinuclidine	4.0	10	CH_2Cl_2	0.61
7	Quinuclidine	8.0	20	CH_2Cl_2	0.49
8	Dabco	2	5	CH_2Cl_2	0.92
9	Dabco	4	10	CH_2Cl_2	0.69
10	Dabco	8	20	CH_2Cl_2	0.39
11	TEA	2	5	CH_2Cl_2	0.94
12	TEA	4	10	CH_2Cl_2	0.90
13	TEA	8	20	CH_2Cl_2	0.79

[cinchonidine] $= 4 \times 10^{-4}$ M, $T = 25$ °C, cell length: 0.2 cm, time mode detection, wavelength: 237.6 nm, Dabco: 1,4-diazabicyclo-[2.2.2]octane, TEA: triethylamine.

we could obtain similar results with the other conformers.[30] In Section 5.3, a procedure (cf. Fig. 5) is described, showing how the stable dimers were searched for.

The characteristic feature of these stable cinchonidine dimer configurations obtained is that the main van der Waals (vdW) bonds formed between the two cinchonidine molecules are between certain partially positive hydrogens of one cinchonidine (mainly on the OH group, but quinoline hydrogen atoms too) and the electron pair on the hybrid p-orbital of the N atom of the other cinchonidine. The N atom can either be a quinoline- or quinuclidine N atom as well. Furthermore, all these stable cinchonidine dimers are bidentate, that is, two of these types of vdW bonds can be found in each of them. Figure 6 shows the four stable cinchonidine dimers we found, while Table 3 summarizes their energetic- and some bonding properties. The '*lower*' cinchonidine of the four dimers exhibited in Figure 6 is about the same orientation toward the viewer. Also, this *lower* cinchonidine has about the same conformation, although not exactly the same, since the other, '*upper*' cinchonidine, places a different influence on it by its different sides or faces. The *lower* cinchonidine is positioned as the quinuclidine part 'hangs' downward from the C9 atom, the quinoline ring is about horizontal, and the OH part is pointing upward. The cinchonidine dimers in Figure 6A are connected to each other via the two quasi-parallel quinoline rings, and between these, two quinoline N···HO vdW bonds are formed. In Section 1, experimental evidence was mentioned, which indicates a parallel quinoline ring arrangement in the dimer of quinine,[7] in accordance with the modeling in this section. In Figure 6B–D the three stable cinchonidine dimers can be originated as follows. An axis can be defined by the OH of the *lower* cinchonidine (pointing upward) and the quinuclidine N atom of the *upper* cinchonidine. It can be imagined as a rotation axis, such the *upper* cinchonidine molecule rotates around it with respect to the standing *lower* cinchonidine. If this *upper* cinchonidine rotates around this axis, three energy minima (the three cinchonidine dimers labeled as B, C, D in Fig. 6) are formed as the *lower* cinchonidine and the *upper* cinchonidine connect via the two main vdW bonds as indicated in Table 3. In Figure 6B, the OH of the *upper* cinchonidine is away, and does not take part in the vdW bond, and its quinoline hydrogens (two) interact with the *lower* cinchonidine quinuclidine N atom. In Figure 6C, the OH moiety of *upper* cinchonidine interacts with the *lower* cinchonidine quinuclidine N atom. Figure 6A and C are comparable in this manner as two quinoline parts are involved in the first, while two quinuclidine parts are involved in the latter (i.e., the same kind of ring systems interact in the two main vdW bonds). In Figure 6D, another energetic minimum forms as the *upper* cinchonidine

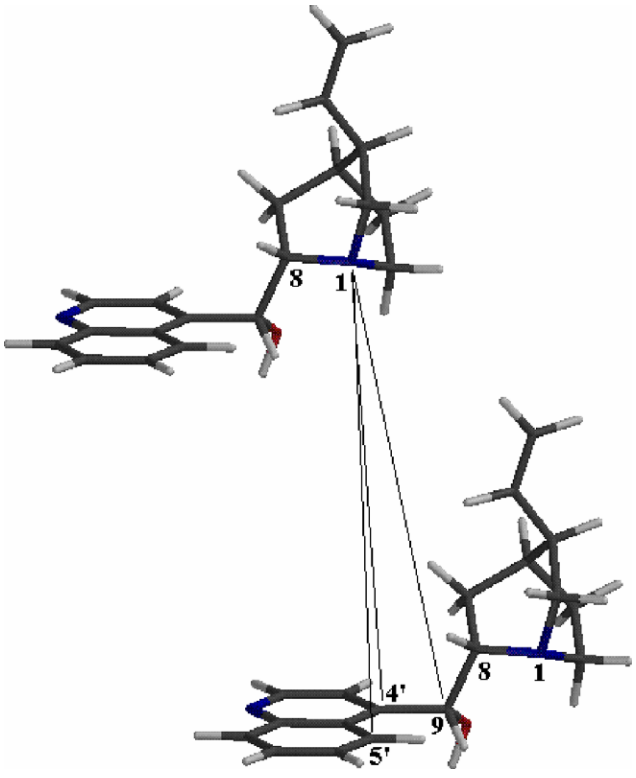

Figure 5. Coordinate system defined and described in the text to generate internal orientations for finding stable cinchonidine dimmers.

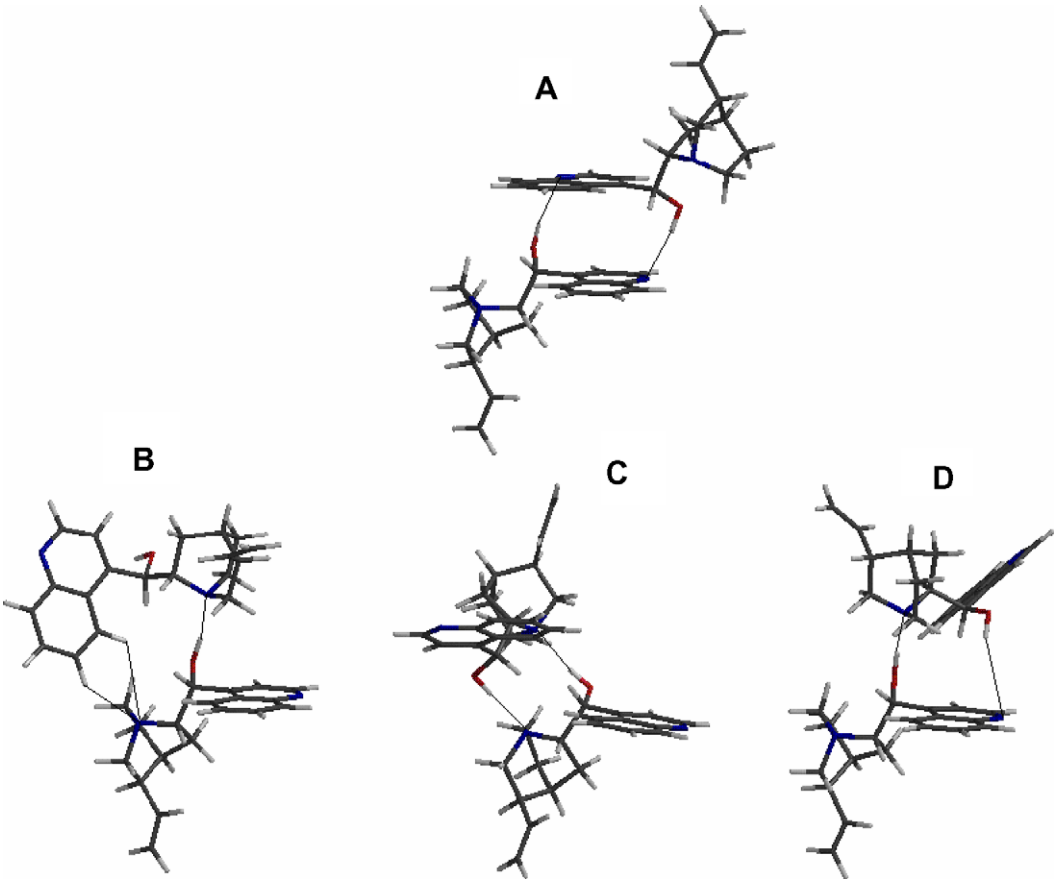

Figure 6. The four stable cinchonidine dimers found. Some of their important properties are summarized in Table 3. Intermolecular vdW bonds between the corresponding atoms are drawn with thin lines.

Table 3. The energetic and bond properties of cinchonidine dimers exhibited in Figure 6

Cinchonidine dimers in Figure 6	Molecular mechanics stabilization energy (kcal/mol)	Ab initio, B3LYP/6-31G* stabilization energy (kcal/mol)	1st main vdW bond	2nd main vdW bond	Note: relative position of the two quinoline rings
A	−16.3 (0.0)	−12.0 (0.0)	Quinoline N···HO	Quinoline N···HO	Quasi parallel
B	−11.9 (4.4)	−12.8 (−0.8)	Quinuclidine N···HO	Quinoline H···quinuclidine N	Quasi-perpendicular
C	−13.2 (3.1)	−12.7 (−0.7)	Quinuclidine N···HO	Quinuclidine N···HO	Quasi-coplanar
D	−12.1 (4.2)	−10.9 (+1.1)	Quinuclidine N···HO	Quinoline N···HO	About 45° angle

The stabilization energy is defined as the 0 K enthalpy of formation of the reaction $2 \times \text{cinchonidine} \rightarrow (\text{cinchonidine})_2$ dimer; the relative energy of the dimer is listed in parentheses with respect to dimer type A.

rotates further, wherein the OH moiety of *upper* cinchonidine interacts with the *lower* cinchonidine quinoline N atom.

Among the dimer types displayed in Figure 6, the 'B' and 'C' forms might provide major contributions to the pattern of the exciton Cotton effects measured in the dichloromethane solution of cinchonidine (Fig. 4a). According to the prediction of the exciton chirality rule, a long-wavelength positive and a short-wavelength negative Cotton bands appear when the electronic transition dipole moments of the interacting chromophores form a positive (clockwise) overlay angle and vice versa. The ^1B_b transition moment of the quinoline moiety is polarized along the long axis of the aromatic ring system and the overlay angles are positive both in the 'B' and 'C' dimers (≈+120° and ≈+80°) but they give negative values in the 'A' and 'D' dimers (≈−20° and ≈−140°).

Interestingly, the four dimers have about the same deep energy minimum on molecular mechanics or B3LYP/6-31G* ab initio level, that is, about 11–13 kcal/mol. This stabilization energy comes from two similar types of vdW bonds, constituted of a partially positive H atom and a filled hybrid p orbital (electron lobe) of an N atom, almost irrespectively of the other closer or further parts of the cinchonidine dimers. In more detail, the dimer in Figure 6A possesses two sp^2 N atoms (in quinoline rings) involved in the two intermolecular bonds with H atoms, while the dimers in Figure 6B and C each possess two sp^3 N atoms

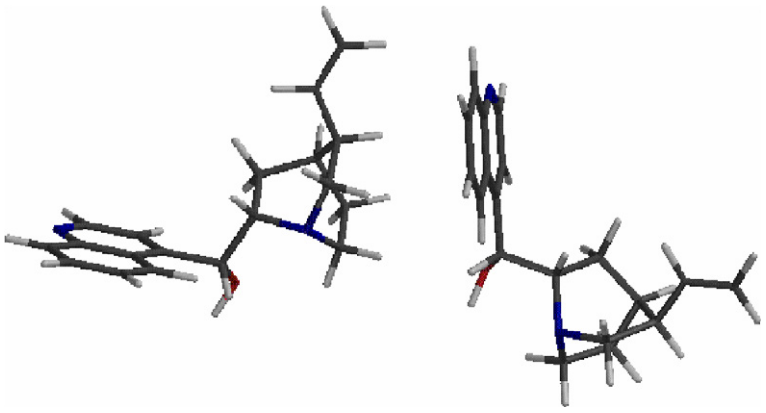

Figure 7. An energetically less stable cinchonidine dimer (see text).

(in quinuclidine rings) in the two intermolecular bonds with H atoms. The former complex (Fig. 6A) is weaker than the latter one (Fig. 6B and C); however, in the former case the two (almost parallel) quinoline rings also interact (i.e., they stabilize the dimer). The net stabilization of the energies are very close to each other in Figure 6A–C.

In addition, the analysis of Figure 6D reveals that the two intermolecular bonds are located between an H atom, an sp^2 N (in quinoline ring) and another H and sp^3 N (in quinuclidine ring). Consequently, this interaction pair is between the two cases described above. However in this dimer, the two quinoline rings do not interact as strongly as in the dimer shown in Figure 6A, but more strongly than in the dimers shown in Figure 6B or C.

Therefore, the net stabilization energy of the dimer shown in Figure 6D is not surprisingly similar to the other dimers depicted in Figure 6. It should be noted, that some less stable cinchonidine dimers may also exist, such as the one shown in Figure 7. There, the positively charged quinuclidine H atoms interacts with the negatively charged quinoline π system of another cinchonidine molecule. The stabilization energy of the dimer exhibited in Figure 7 is only about −3 kcal/mol, that is, much weaker than the four displayed in Figure 6.

4. Conclusion

Experimental evidences have been reported, supporting the suggestions made earlier that cinchonidine can exist in its dimer form in the liquid phase in enantioselective hydrogenation experiments. The so-called 'ATA effect' is attributed to breaking the cinchonidine dimers in liquid phase resulting in a virtual increase of cinchonidine concentration. As a consequence, the ee and the rate also increase. Upon using circular dichroism spectroscopy further evidences were obtained for the suppression of dimer formation in the presence of ATAs in aprotic solvents. Upon using ethanol as a solvent or MeO-cinchonidine as chiral modifier the Cotton effect characteristic for the formation of dimer was not observed. The cinchonidine dimers were modeled computationally resulting in four dimers, which were described energetically as well as with some important bond characteristics. We have found that two vdW bonds are formed in each types of dimer, mainly between the OH of one and the electron lobe of N atom on the other cinchonidine.

5. Experimental

5.1. Hydrogenation of ethyl pyruvate

The catalytic runs were carried out as described earlier,[13,31] using a commercial 5% Pt/Al_2O_3 (E4759) catalyst and solvents (toluene, methylcyclohexane, and ethanol) from Reanal. The cinchonidine chiral modifier and ATAs (quinuclidine, 3-quinuclidinol, Dabco, MPD, TEA, Edcha, Edipa) were purchased from Fluka. MeO-cinchonidine was prepared according to the literature.[32] The EtPy (Fluka) was freshly distilled before each catalytic experiment. Hydrogenation of the substrate was carried out in an SS-autoclave at a rate of agitation of 500 rpm and at 10–50 bar hydrogen pressures. The reaction temperature was 20 °C in all experiments. Injection or premixing techniques was used to introduce the chiral modifier into the reactor[13] ATAs were injected or premixed together with cinchonidine (coinjection and copremixing, respectively). Samples were taken at different reaction times and analyzed by a GC using a capillary column (Chiraldex B-TA, 0,25 mm, 30 m) and flame ionization detector. Using the known definition of enantioselectivity as $ee = ([R - S]/[R + S])$, the ee_{max} is defined as the highest enantiomeric excess value measured in a given reaction. The ee_{end} values were measured at the end of the reaction, that is, after 90 min. The ee values in the conversion had a relative reproducible error of approximately 5%. The kinetic curves of the enantioselective hydrogenation followed the characteristic two step behavior as described earlier.[13,30] First order rate constants were calculated from experimental points measured in the first 10 min and between 25 and 60 min (k_1, k_2, respectively). These values were used to compare the catalytic activity under various experimental conditions. The k values were reproducible within 10% providing the same batch of EtPy.

5.2. Circular dichroism measurements

Circular dichroism spectra were measured at 25 °C using a Jasco J-715 spectropolarimeter. The concentration of cinchonidine and the cell length was 4×10^{-4} M and 0.2 cm, respectively, in all experiments. The spectra were signal-averaged three times with a bandwidth of 1.0 nm and a resolution of 0.2 nm at a scan speed of 50 nm/min. The spectropolarimeter records the cinchonidine data as ellipticity ('Θ') in units of millidegrees (mdeg). The quantity of 'Θ' is converted to '$\Delta\varepsilon$' values using the equation of $\Delta\varepsilon = \Theta/(33{,}982cl)$, where '$\Delta\varepsilon$' is the molar circular dichroic absorption coefficient expressed in $M^{-1}\,cm^{-1}$, 'c' is the concentration of the sample solution expressed in mol/L, and 'l' is the path length in cm. Dichloromethane and ethanol were used as a solvent. Time mode detection at a wavelength of 237.6 nm was applied.

5.3. Computation

A silicon graphics (Octan 8, 175 MHz, IRIX 6.5 environment) machine was used for Spartan molecular building and molecular mechanics calculations[33] and a 2 GHz PC with LINUX environment (with 40GB disc space) for the ab initio calculations with Gaussian program package.[34] These computational tools were used for the required modeling in this work for all molecules: cinchonidine and its dimers in free space (or gas phase). For correlation calculations [necessary for the chemical accuracy (1 kcal/mol)] the popular perturbation MP2 (Moller–Plesset of 2nd order) method,[33] which provides remarkable results for π–π interactions or for the vdW intermolecular forces between molecules, could not be employed for these large cinchonidine dimers due to a convergence problem as well as a disc space shortage. However, the density functional theory (DFT) method B3LYP (Becke 3–Lee–Young–Parr)[34] on 6-31G* computational basis level was easily accessible. For this reason we used the latter method of calculation for the modeling.

The molecular building and search of the cinchonidine dimers discussed in Section 3 was as follows: to orientate two cinchonidine molecules relative to each other, we have used the help of its dipole moment vector as well as some of its atoms. In Figure 5, the C4′, C5′, C9 atoms of the lower and N1 atom of the upper cinchonidine were used to define an internal coordinate system (see thin lines). The C5′–C4′–C9 atoms roughly form a 90° angle. The middle one, C4′, connecting the quinoline to the C9 atom, can be considered like an origin of a Cartesian coordinate system. The atoms C5′, C9, and N1 (upper) can be considered as points lying on the x, y, and z axes of this Cartesian coordinate system, respectively. The N1 atom of the *upper* cinchonidine was moved around the surface of a hypothetical sphere around the *lower* cinchonidine being concentric with the origin (C4′ atom) of this Cartesian coordinate system defined. In this way the tetrahedrons, defined with corner atoms C4′, C5′, C9, and the upper N1, were transformed as the upper N1 changed positions and the others were fixed. The angles, which varied in the transformation in this tetrahedron had the step size of about 40°. Technically, the positions of the upper N1 atom around the lower cinchonidine were lying on a projected, zoomed-out hypothetical sphere, and 60 points were selected at about equal spacing on that surface. For example, the upper N1–lower C4′ distance was about 7 Å (radius of the sphere), and the distance between the two closest hydrogen atoms were about 2–2.5 Å. This provided vdW interactions between the two cinchonidine molecules, so the system could be relaxed with molecular mechanics. The dipole moment vector is approximately along the N1→C8 bond of the *lower* molecule or, similarly, the corresponding one in the *upper* molecule. All the 60 points above were multiplied by the parallel and anti-parallel positions of these dipole moment vectors (flipping the *upper* cinchonidine). Furthermore, with the help of two atoms from the *lower* cinchonidine and two atoms from the *upper* cinchonidine, a dihedral angle, (lower N1)–(lower C8)–(upper N1)–(upper C8), was also defined and scanned the range from −180° to 180° with the step of 30° (rotating the upper cinchonidine). This also multiplied the initial configurations described above. With these many initial relative configurations, the two cinchonidine molecules were relaxed by Spartan molecular mechanics, and a few characteristic stable dimer configurations were obtained. These are described and analyzed in Section 3.

Acknowledgments

The authors wish to thank the Engelhard Corp. for providing the catalyst (E4759) as a gift. We also thank Dr. András Gergely (Institute of Pharmaceutical Chemistry, Semmelweiss University, Budapest) for his help in the circular dichroism measurements.

References

1. Wynberg, H. In *Topics in Stereochemistry*; Eliel, E. L., Wilen, S. H., Allinger, N. L., Eds.; Asymmetric Catalysis by Alkaloids; Wiley: New York, 1986; Vol. 16, pp 87–126.
2. Kacprzak, K.; Gawronski, J. *Synthesis* **2001**, 961–998.
3. Oleksyn, B. J. *Acta Crystallogr., Sect. B* **1982**, *38*, 1832–1834.
4. Gawronsky, J.; Brzostowska, M.; Koput, J. *Croat. Chem. Acta* **1989**, *62*, 97–107.
5. Hiemstra, H.; Wynberg, H. *J. Am. Chem. Soc.* **1981**, *103*, 417–430.
6. Williams, T.; Pitcher, R. G.; Bommer, P.; Gutzwiller, J.; Uskokovic, M. R. *J. Am. Chem. Soc.* **1969**, *91*, 1871–1872.
7. Ucello-Barretta, G.; Di Bari, L.; Salvadori, P. *Magn. Reson. Chem.* **1992**, *30*, 1054–1063.
8. Bartók, M.; Szabó, P. T.; Bartók, T.; Szöllősi, Gy. *Rapid Commun. Mass Spectrom.* **2000**, *14*, 509–514.
9. Ferri, D.; Bürgi, T.; Baiker, A. *J. Chem. Soc., Perkin Trans. 2* **1999**, 1305–1311.
10. Wesełucha-Birczyńska, A. *Vib. Spectrosc.* **2004**, *35*, 189–198.
11. Orito, Y.; Imai, S.; Niwa, S. *J. Chem. Soc. Jpn.* **1979**, 1118–1120.
12. Studer, M.; Blaser, H. U.; Exner, C. *Adv. Synth. Catal.* **2003**, *345*, 45–65.
13. Margitfalvi, J. L.; Tálas, E.; Tfirst, E.; Kumar, C. V.; Gergely, A. *Appl. Catal.* **2000**, *191*, 177–191.
14. Bartók, M.; Bartók, T.; Szöllősi, Gy.; Felföldi, K. *Catal. Lett.* **1999**, *61*, 57–60.

15. Tálas, E.; Botz, L.; Margitfalvi, J.; Sticher, O.; Baiker, A. *J. Planar Chromatogr.* **1992**, *5*, 28–34.
16. Morawsky, V.; Prüsse, U.; Witte, L.; Vorlop, K. D. *Catal. Commun.* **2000**, *1*, 15–20.
17. Szöllősi, Gy.; Forgó, P.; Bartók, M. *Chirality* **2003**, *15*, S82–S89.
18. Blaser, H. U.; Jalett, H. P.; Lottenbach, W.; Studer, M. *J. Am. Chem. Soc.* **2000**, *122*, 12675–12682.
19. Garland, M.; Blaser, H. U. *J. Am. Chem. Soc* **1990**, *112*, 7048–7050.
20. Huck, W. R.; Bürgi, T.; Mallat, T.; Baiker, A. *J. Catal.* **2003**, *216*, 276–287.
21. Nitta, Y. *Chem. Lett.* **1999**, 635–636.
22. Nitta, Y. *Top. Catal.* **2000**, *13*, 179–185.
23. Margitfalvi, J. L.; Tálas, E.; Hegedűs, M. *Chem. Commun.* **1999**, 645–646.
24. Margitfalvi, J. L.; Tálas, E.; Marín-Astorga, N.; Marzialetti, T. In *Influence of Achiral Tertiary Amines on the Enantioselective Hydrogenation of α,β-Diketones over Cinchonidine–Pt/Al_2O_3 Catalyst*; Sowa, J., Ed.; Chemical Industries, Catalysis of Organic Reactions; Taylor & Francis: New York, 2005; pp 535–540.
25. Rylander, P. N. *Catalytic Hydrogenation in Organic Syntheses*; Academic Press: New York, 1979.
26. Jenkins, D. J.; Alabdulraham, A. M. S.; Attard, G. A.; Griffin, K. G.; Johnston, P.; Wells, P. B. *J. Catal.* **2005**, *234*, 230–239.
27. Bonello, J. M.; Lambert, R. M.; Künzle, N.; Baiker, A. *J. Am. Chem. Soc.* **2000**, *122*, 9864–9865.
28. Blaser, H.-U.; Jalett, H. P.; Monti, D. M.; Baiker, A.; Wehrli, J. T. *Stud. Surf. Catal.* **1991**, *61*, 147–153.
29. Bürgi, T.; Baiker, A. *J. Am. Chem. Soc.* **1998**, *120*, 12920–12926.
30. Margitfalvi, J. L.; Tfirst, E. *J. Mol. Catal. A: Chem.* **1999**, *139*, 81–95.
31. Margitfalvi, J. L.; Hegedűs, M. *J. Mol. Catal. A: Chem.* **1996**, *107*, 281–289.
32. Borszeky, K.; Bürgi, T.; Zhaohui, Z.; Mallat, T.; Baiker, A. *J. Catal.* **1999**, *187*, 160–166.
33. Hehre, W. J.; Huang, W. W.; Klunzinger, P. E.; Deppmeier, B. J.; Driessen, A. J. Spartan Manual, Wavefunction, 18401 Von Karman Ave., Suite 370, Irvine, CA 92612.
34. Frisch, M. J.; Trucks, G. W.; Schlegel, H. B.; Scuseria, G. E.; Robb, M. A.; Cheeseman, J. R.; Zakrzewski, V. G.; Montgomery, J. A., Jr.; Stratmann, R. E.; Burant, J. C.; Dapprich, S.; Millam, J. M.; Daniels, A. D.; Kudin, K. N.; Strain, M. C.; Farkas, O.; Tomasi, J.; Barone, V.; Cossi, M.; Cammi, R.; Mennucci, B.; Pomelli, C.; Adamo, C.; Clifford, S.; Ochterski, J.; Petersson, G. A.; Ayala, P. Y.; Cui, Q.; Morokuma, K.; Malick, D. K.; Rabuck, A. D.; Raghavachari, K.; Foresman, J. B.; Cioslowski, J.; Ortiz, J. V.; Stefanov, B. B.; Liu, G.; Liashenko, A.; Piskorz, P.; Komaromi, I.; Gomperts, R.; Martin, R. L.; Fox, D. J.; Keith, T.; Al-Laham, M. A.; Peng, C. Y.; Nanayakkara, A.; Gonzalez, C.; Challacombe, M.; Gill, P. M. W.; Johnson, B. G.; Chen, W.; Wong, M. W.; Andres, J. L.; Head-Gordon, M.; Replogle, E. S.; Pople, J. A. GAUSSIAN *98, Revision A.7*; Gaussian: Pittsburgh, PA, 1998.